nature neuroscience

Topographical representation of odor hedonics in the olfactory bulb

Florence Kermen[1,3,4], Maëllie Midroit[1,4], Nicola Kuczewski[1], Jérémy Forest[1], Marc Thévenet[1], Joëlle Sacquet[1], Claire Benetollo[2], Marion Richard[1], Anne Didier[1,5] & Nathalie Mandairon[1,5]

Hedonic value is a dominant aspect of olfactory perception. Using optogenetic manipulation in freely behaving mice paired with immediate early gene mapping, we demonstrate that hedonic information is represented along the antero-posterior axis of the ventral olfactory bulb. Using this representation, we show that the degree of attractiveness of odors can be bidirectionally modulated by local manipulation of the olfactory bulb's neural networks in freely behaving mice.

In all species, including humans, odors strongly impact behavior. Besides odor identity, the hedonic value or pleasantness of an odor is an important variable for smell-triggered behaviors, for example, approaching or avoiding an odor source. The hedonic value or attractiveness of an odorant is thus recognized as the dominant aspect of olfactory perception[1,2]. While experience and culture shape odor hedonics[3,4], spontaneous attraction or avoidance is also observed for unfamiliar odorants[5], suggesting an innate component. This raises the issue of the representation of naive hedonic tone in the brain.

Odor signals are received by odorant receptors expressed by sensory neurons in the olfactory epithelium and can be represented as an odor map in the glomerular layer of the olfactory bulb[6]. Although glomerular maps in the dorsal olfactory bulb have been shown to represent the aversive properties of some odorants[7–9], it remains unclear whether bulbar maps represent innate positive versus negative hedonic tones. In this study, we combine immediate early gene mapping[7] and optogenetics to show that the degree of behavioral attraction to an odorant is represented along the antero-posterior axis of the ventral olfactory bulb, suggesting a functional organization for innate hedonic value.

To determine which odorants trigger innate positive or negative hedonic tone in mice, we tested the olfactory preferences of 50 mice for a set of 16 odorants with a wide range of molecular properties (**Supplementary Table 1** and **Supplementary Fig. 1**), chosen to be unfamiliar to the mice, with no particular biological significance. Odorant investigation time, assessed as an index of attractiveness[7,10], differed significantly across the odorants (permutation test $P = 0.034$; **Fig. 1**).

We selected the five most investigated (camphor, limonene, β-ionone, citronellol and cineole) and the five least investigated (pyridine, thioglycolic acid, 3-hexanol, guaiacol and *p*-cresol) odorants and compare their investigation times to those for 2,3,5-trimethyl-3-thiazoline (TMT) and mouse urine, which are recognized as being, respectively, aversive and attractive to mice (**Supplementary Fig. 2a**). Time spent investigating the five least explored odorants was different from that spent investigating urine, and time spent investigating the five most explored was different from that for TMT, suggesting that the mice found these odorants respectively aversive and attractive. The speed of approach to the odorized hole was closely correlated to investigation time, further strengthening investigation time as a measure of attractiveness (**Supplementary Fig. 2b**,**c**).

In the olfactory bulb, spatially organized incoming information[6] is transferred to mitral/tufted (M/T) cells, which are the olfactory bulb's relay cells. M/T cell activity is shaped by complex interactions with superficial and deep interneurons, the periglomerular and granule cells, respectively[11]. *Zif268* expression in olfactory bulb interneurons allows mapping of odor-evoked activation in response to odor stimulation[7,12–15]. To reveal the activation patterns that reflect the attractiveness of the odors independently of their identity, we averaged the activation evoked by each of the five most and the five least attractive odorants (**Fig. 2**). The overall densities of Zif268-expressing cells were similar between both groups and layers (Mann-Whitney $P = 0.89$ for glomerular and $P = 0.53$ for granule cell layers; **Fig. 2a**,**b**). However, differences in the spatial distribution of the odor-responding cells accounted for the innate attraction mice had to the odors. We constructed Zif268$^+$ cell maps by extracting labeled-cell density from 36 sectors in the glomerular and granule cell layers along the antero-posterior axis of the olfactory bulb. These density values were then reported in 2D maps in which each column corresponded to one olfactory bulb section and each bin corresponded to the labeled-cell density in one sector[14,15] (**Fig. 2c**). Compared to pleasant odorants, unpleasant odorants led to a higher density of activated cells in the ventro-posterior glomerular and granule cell layers of the olfactory bulb. In the dorsal olfactory bulb, the response to unpleasant odorants was mostly posterior in the glomerular layer (**Fig. 2d**,**e**, **Supplementary Figs. 3** and **4**, and **Supplementary Tables 2** and **3**). In contrast, pleasant odorants evoked higher activity in the antero-ventral area of both the glomerular and granule cell layers (**Fig. 2d**,**e**, **Supplementary Figs. 3** and **4**, and **Supplementary Tables 2** and **3**).

Analysis of overlaps between the odorant-specific maps within each hedonic group yield maps resembling the across-odorant averaged maps, supporting the idea that the latter reflect activation features common to pleasant or unpleasant odorants rather than activation features of individual odorants (**Supplementary Figs. 3d**,**e** and **5**).

In summary, while the responsiveness of the dorsal glomerular layer to unpleasant odorant has been documented[7], the substantial modulations of Zif268 expression between pleasant and unpleasant

[1]INSERM, U1028, CNRS, UMR5292, Lyon Neuroscience Research Centre, Neuroplasticity and Neuropathology of Olfactory Perception Team, University Lyon 1, University of Lyon, Lyon, France. [2]INSERM, U1028, CNRS, UMR5292, Lyon Neuroscience Research Center, Neurogenetic and Optogenetic Platform, University Lyon 1, University of Lyon, Lyon, France. [3]Current address: Kavli Institute for Systems Neuroscience, Centre for Neural Computation, The Faculty of Medicine, NTNU, Trondheim, Norway. [4]These authors contributed equally to this work. [5]These authors jointly supervised this work. Correspondence should be addressed to N.M. (nathalie.mandairon@cnrs.fr).

Received 4 March; accepted 29 April; published online 6 June 2016; doi:10.1038/nn.4317

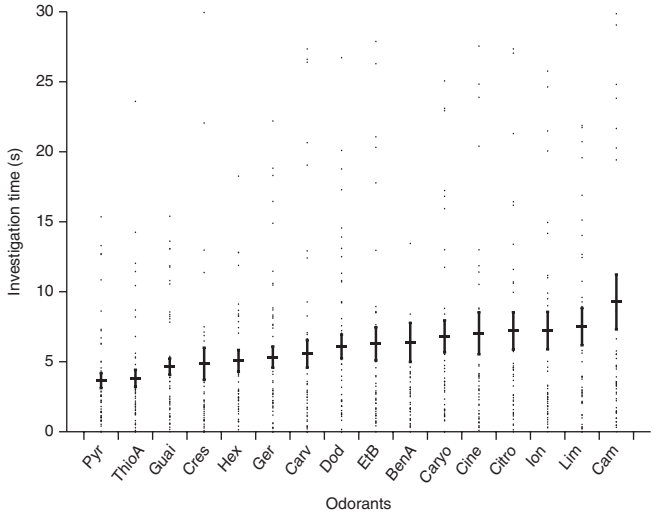

Figure 1 Mice displayed various levels of innate attraction for odorants. Investigation times, automatically measured on a one-hole-board apparatus during 2-min tests, vary for the 16 odorants: pyridine (Pyr), thioglycolic acid (ThioA), guaiacol (Guai), *p*-cresol (Cres), 3-hexanol (Hex), geraniol (Ger), D-carvone (Carv), dodecanal (Dod), ethyl butyrate (EtB), benzyl acetate (BenA), β-caryophyllene (Caryo), cineole (Cine), citronellol (Citro), β-ionone (Ion), limonene (Lim) and camphor (Cam). Odor effect, $F_{(15,735)} = 1.76$, permutation test $P = 0.034$, $n = 50$ mice. Data are represented as mean ± s.e.m. and individual data points. For clearer representation, 20 data points (out of 800) above 30 s are not shown and are distributed as follows: Cres 2; Hex 1; EtB 1; BenA 5; Caryo 2; Cine 1; Citro 1; Ion 2; Lim 2; Cam 3.

odorants were found mostly along the antero-posterior axis of the ventral olfactory bulb.

Because granule cells shape M/T cell activity and therefore the output message read by higher olfactory structures, we hypothesized that changing the output message of the M/T cells by manipulating inhibition should directly affect behavior. We used optogenetic inhibition of localized populations of granule cells with the aim of disinhibiting M/T cells. We achieved this by infusing a lentivirus allowing halorhodopsin-EYFP (enhanced yellow fluorescent protein) expression in neurons (Lenti-hSyn-NpHR-EYFP, NpHR (*Natronomonas* halorhodopsin)) into the postero-ventral or antero-ventral granule cell layer (**Supplementary Fig. 6**). Control animals were infused with an empty lentivirus (Lenti-hSyn-EYFP, control-EYFP). We confirmed that EYFP$^+$ cell density was always higher in the areas targeted by virus infusions compared to non-targeted regions (**Supplementary Fig. 6a**,**b**). In addition, viral diffusion was limited to the granule cell layer as only 0.38% of EYFP$^+$ cells were M/T cells identified by the expression of their specific marker Tbx21 (7,537 M/T cells counted). Light stimulation was effective since it induced a decrease in the number of cells coexpressing EYFP and Zif268 (**Supplementary Figs. 6c** and **7**) and in total Zif268$^+$ cell density (**Supplementary Fig. 6d**). Such differences were not observed in mice infused with the empty virus. Furthermore, light stimulation in olfactory bulb slices inhibited firing in granule cells expressing NpHR but not in those expressing EYFP in the control animals (**Supplementary Fig. 8a**). In addition, using cell-attached recording of M/T cells in olfactory bulb slices, we showed that light-stimulation of granule cells disinhibits M/T cell activity in NpHR infused mice compared to controls (32.88 ± 10.05% of difference between the controls and NpHR, one-sample *t*-test $P = 0.022$). Similarly, postmortem quantification of Zif268 expression in M/T cells showed disinhibition in light-targeted compared to non-light-targeted regions (**Supplementary Fig. 8b**,**c**).

Optogenetic inactivation of transduced neurons was achieved in freely behaving mice during preference testing by automatically triggering a light stimulation each time the animal approached the odorized hole. In the groups with postero-ventral viral infusion, the investigation time for the five unpleasant odorants was increased under posterior light stimulation in the NpHR group compared to the control-EYFP group, showing a shift toward an increased attractiveness of these odorants (**Fig. 3a** and **Supplementary Fig. 9a**). The investigation time of pleasant odorants was unchanged (**Fig. 3c** and **Supplementary Fig. 9c**). Following viral infusion in the antero-ventral olfactory bulb, light-triggered inactivation of this region decreased the investigation time for the five attractive odorants in the NpHR group compared to that of the control-EYFP group, suggesting a shift toward

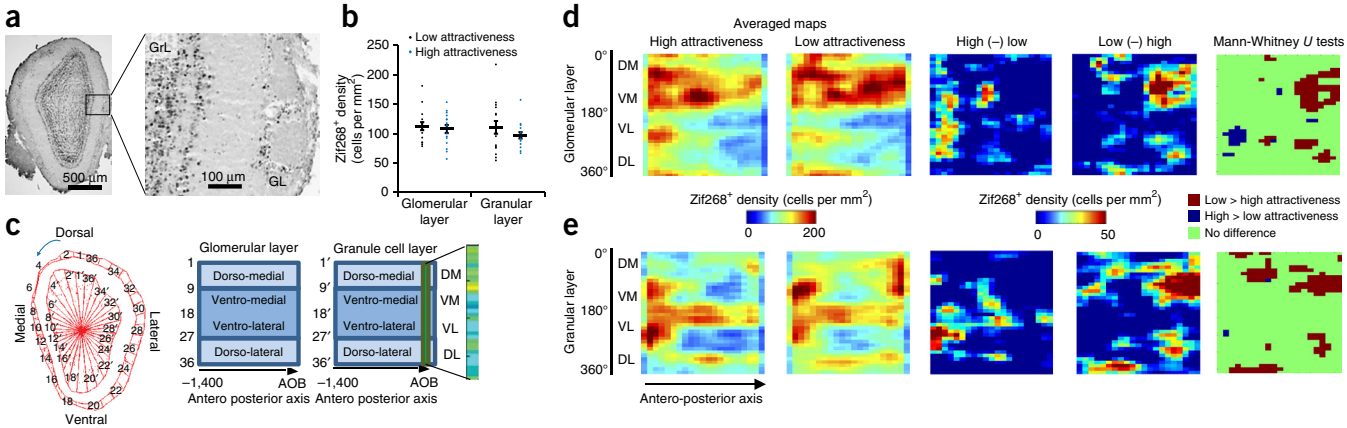

Figure 2 Pleasant and unpleasant odorants evoke different patterns of olfactory bulb activation. (**a**) Coronal sections of the olfactory bulb showing Zif268 labeling (representative of 32 animals) in granular layer (GrL) and glomerular layer (GL). (**b**) Zif268$^+$ cell density is similar in response to unattractive and highly attractive odorants (Mann-Whitney, $P = 0.89$ for glomerular and $P = 0.53$ for granule cell layers; $n = 16$ mice per group) (mean ± s.e.m. and individual data points). (**c**) Cell mapping method. Every Zif268$^+$ cell was counted on each sampled section. Density of labeled profiles was extracted from 36 sectors of 10° of the granule or periglomerular cell layer. For each layer, the cell densities were reported into a matrix in which one column represented all the sectors of one section. (**d**) Left, Zif268$^+$ cell density maps in the glomerular layer in response to high- or low-attractiveness odorants. Middle, subtraction maps. Right, false discovery rate–corrected Mann-Whitney point-to-point comparisons. Significance cutoff was set at $P < 0.05$. (**e**) Same as **d** for the granule cell layer. AOB, accessory olfactory bulb; DM, dorso-medial; VM, ventro-medial; VL, ventro-lateral; DL, dorsolateral.

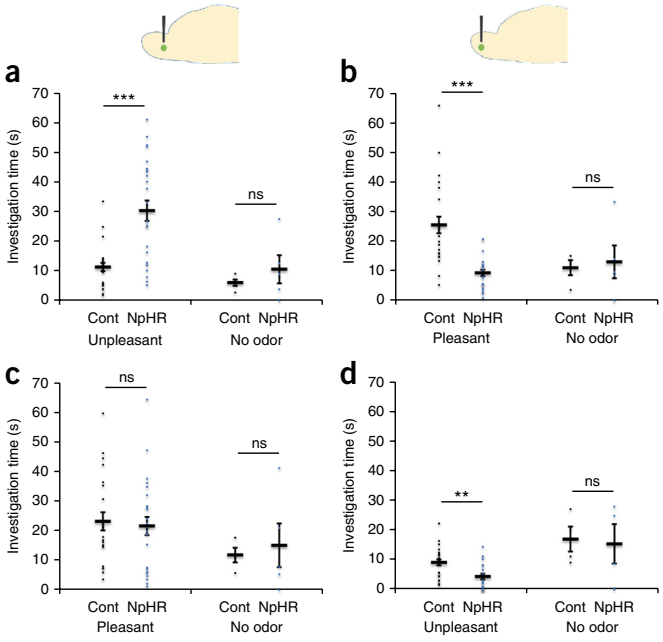

Figure 3 Behavioral effect of optogenetic stimulation. The investigation time of the odorants after postero-ventral (left diagram, **a** and **c**) or antero-ventral (right diagram, **b** and **d**) light stimulation in NpHR-infused (NpHR, blue) and control virus-infused (Cont, black) mice. 5 unpleasant odorants ($n = 5$ mice per odorant), 5 pleasant odorants ($n = 5$ mice per odorant) and one no- (zero-) odorant condition tested. Mann-Whitney group effect; **a**, $P = 0.00008$; **b**, $P = 0.000001$; **c**, $P = 0.75$; **d**, $P = 0.0014$ (mean ± s.e.m. and individual data points); n.s., non-significant.

a reduced attractiveness of the odorants (**Fig. 3b** and **Supplementary Fig. 9b**). Anterior light stimulation further reduced the attractiveness of the unpleasant odorants (**Fig. 3d** and **Supplementary Fig. 9d**). In this optogenetic experiment, the overall increase in investigation time compared to **Figure 1** can be explained by the smaller number of odors experienced by the animals. The effects of light were dependent on sensory stimulation since light stimulation in the absence of the odorant had no behavioral effect.

Inhibition of the anterior olfactory bulb thus produces a reduction in investigation time regardless of odorant attractiveness. This may be due to an increased relative salience of the activity in the posterior olfactory bulb highlighting the role of posterior olfactory bulb activity in encoding odorant unpleasantness. Inhibition of the posterior olfactory bulb failed to further increase the attractiveness of pleasant odorants. This is consistent with the lower level of activity observed in the posterior olfactory bulb in response to pleasant odorants.

In summary, we have demonstrated the presence of a neural trace for positive and negative hedonic tones of odors along the antero-posterior axis of the olfactory bulb. Local optogenetic manipulation of this neural hedonic signature changed the behavioral response to odorants, suggesting that bulbar representations give a reliable indication of the level of odor attractiveness. Even though the degree of attraction to an odor was innate in our mice (i.e., not trained), we were able to modify this by modulating neural activity. Adding to previous experiments showing that aversion to an odor can be abolished by removing specific glomeruli[7], we show here that innate attractiveness is represented along an anatomical axis of the olfactory bulb and that this could be subject to plasticity as it can be modulated by changes in inhibitory activity. Whether this representation of hedonics along the olfactory bulb results from organized projections of olfactory sensory neurons recognizing specific molecular features of pleasant or unpleasant odorants remains unknown but is supported by evidence for a spatial representation of hedonics in the main olfactory epithelium[16]. Finally, it remains to be determined how hedonic-dependent activity in the olfactory bulb is interpreted by higher olfactory structures. M/T cells project to different targets according to their position along the antero-posterior axis, determined by their ontogenetic birth date[17]. Several candidate structures respond to odorant hedonics[18,19], and it would thus be interesting to look for differential projections from anterior and posterior regions of the olfactory bulb to these olfactory brain regions.

METHODS

Methods and any associated references are available in the online version of the paper.

Note: Any Supplementary Information and Source Data files are available in the online version of the paper.

ACKNOWLEDGMENTS

We thank G. Froment, D. Nègre and C. Costa from the lentivector production facility at SFR BioSciences de Lyon (UMS3444/US8); A. Fleischmann and I. Vieira for their help with the optogenetic set up; P. Fonlupt for his help with the statistical analysis; Y. Yoshihara (Riken Brain Science Institute, Saitama, Japan) for the gift of the Tbx21 antibody and C. Linster, M. Bensafi and A. Fournel for their helpful comments on the manuscript. This work was supported by the CNRS, INSERM, Lyon 1 University, the Roudnitska Foundation (fellowship to M.M.) and the French Ministry for Research and Ecole Normale Supérieure de Lyon (fellowship to F.K.).

AUTHOR CONTRIBUTIONS

F.K., A.D. and N.M. conceived the experiments; F.K., M.M., N.K., J.F., J.S. and N.M. performed the experiments; C.B. and M.R. engineered the lentiviruses; F.K., M.M., M.T., A.D., M.T., N.K. and N.M. analyzed the data and F.K., M.M., M.R., A.D. and N.M. wrote the article.

COMPETING FINANCIAL INTERESTS

The authors declare no competing financial interests.

1. Richardson, J.T. & Zucco, G.M. *Psychol. Bull.* **105**, 352–360 (1989).
2. Yeshurun, Y. & Sobel, N. *Annu. Rev. Psychol.* **61**, 219–241 (2010).
3. Barkat, S., Poncelet, J., Landis, B.N., Rouby, C. & Bensafi, M. *Neurosci. Lett.* **434**, 108–112 (2008).
4. Yeomans, M.R., Mobini, S., Elliman, T.D., Walker, H.C. & Stevenson, R.J. *J. Exp. Psychol. Anim. Behav. Process.* **32**, 215–228 (2006).
5. Mandairon, N., Poncelet, J., Bensafi, M. & Didier, A. *PLoS One* **4**, e4209 (2009).
6. Mori, K. & Sakano, H. *Annu. Rev. Neurosci.* **34**, 467–499 (2011).
7. Kobayakawa, K. *et al. Nature* **450**, 503–508 (2007).
8. Takahashi, Y.K., Nagayama, S. & Mori, K. *J. Neurosci.* **24**, 8690–8694 (2004).
9. Johnson, M.A. *et al. Proc. Natl. Acad. Sci. USA* **109**, 13410–13415 (2012).
10. Mandairon, N. *et al. J. Neurosci. Methods* **180**, 296–303 (2009).
11. Nagayama, S., Homma, R. & Imamura, F. *Front. Neural Circuits* **8**, 98 (2014).
12. Inaki, K., Takahashi, Y.K., Nagayama, S. & Mori, K. *Eur. J. Neurosci.* **15**, 1563–1574 (2002).
13. Mandairon, N., Didier, A. & Linster, C. *Neurobiol. Learn. Mem.* **90**, 178–184 (2008).
14. Moreno, M.M. *et al. J. Neurosci.* **32**, 3748–3758 (2012).
15. Mandairon, N. *et al. Eur. J. Neurosci.* **24**, 3578–3588 (2006).
16. Lapid, H. *et al. Nat. Neurosci.* **14**, 1455–1461 (2011).
17. Imamura, F., Ayoub, A.E., Rakic, P. & Greer, C.A. *Nat. Neurosci.* **14**, 331–337 (2011).
18. Gadziola, M.A., Tylicki, K.A., Christian, D.L. & Wesson, D.W. *J. Neurosci.* **35**, 4515–4527 (2015).
19. Li, Q. & Liberles, S.D. *Curr. Biol.* **25**, R120–R129 (2015).

ONLINE METHODS

Animals. 125 adult male C57Bl6/J mice (Charles River Laboratories, L'Arbresle, France) aged 2 months at the beginning of the experiments were used. Experiments were done following procedures in accordance with the European Community Council Directive of 22nd September 2010 (2010/63/UE) and the National Ethics Committee (Agreement DR2013-48 (vM)). Mice were housed in groups of five in standard laboratory cages and were kept on a 12 h light/dark cycle (at a constant temperature of 22 °C) with food and water ad libitum. Behavioral experiments started not earlier than a week after the arrival of the animals and were conducted in the afternoon (2–6 p.m., light phase).

Odorants. 16 monomolecular odorants were selected based on molecular diversity (**Supplementary Fig. 1**). To avoid differences in the concentration of these odorants in the inhaled air due to differences in their volatility, they were diluted in mineral oil so as to achieve an approximate gas-phase partial pressure of 1 Pa (ref. 20; **Supplementary Table 1**). Vapor pressure values were collected from http://www.thegoodscentscompany.com. 2,3,5-Trimethyl-3-thiazoline (TMT, Contech, Canada) and urine from female mice were also used.

Olfactory preference testing. Odor attractiveness was measured using odor investigation time (n = 50 mice). We used a computer-assisted one-hole-board apparatus fitted with sensors to automatically monitor the duration of nose-poking into the central hole[5,10]. A polypropylene swab impregnated with 60 µl of the odorant (1 Pa) was placed at the bottom of the hole, under a grid covered with clean bedding. Every animal was allowed to explore each of the 16 odorants for 2 min. The bedding was replaced after each trial. Total duration of nose-poking into the hole (odor investigation time) was used as a measure of odor preference. Each animal tested one odorant per d. Odorants were randomly presented and animals performed no more than 3 consecutive d of testing. The effect of the odorants on investigation time was analyzed by random permutation test (10 series of 10,000 permutations). This experiment was repeated using 30 additional mice using the 5 most and 5 least explored odorants and investigation times were compared to those for TMT (0.004% in propylene glycol, 60 µl) and urine (20 µl). In this second experiment, we also noted the time elapsed for the mouse's nose to cross the distance of 2 cm around the hole (from which we calculated the speed of approach to the hole) using custom-made video tracking software (n = 15 mice; Volcan) as well as the investigation time of the odorant.

Odorant stimulation, immunohistochemistry and labeled cell mapping. *Odorant selection.* The 5 most attractive odorants, i.e., the most explored (camphor, limonene, β-ionone, citronellol and cineole) and the 5 least attractive, i.e., the least explored (pyridine, thioglycolic acid, 3-hexanol, guaiacol and *p*-cresol), were used for odorant stimulation. The mice were randomly assigned to each odorant.

Odor stimulation and euthanasia. The mice were first placed in individual clean cages for 1 h, with an empty tea ball hanging from the top of the cage. A polypropylene swab impregnated with the odorant (60 µl, 1Pa) was then placed in the tea ball for a further hour. One hour after the end of stimulation, the mice were deeply anaesthetized (pentobarbital, 0.2 ml/30 g) and killed by intracardiac perfusion of 50 ml of fixative (PFA 4%, pH = 7.4). This 1-h delay has previously been shown to enable the expression of Zif268 in response to odorant stimulation[21]. The brains were removed, post-fixed overnight, cryoprotected in sucrose (20%), frozen rapidly and then stored at −20 °C before sectioning at 14 µm with a cryostat.

Immunohistochemistry. The Zif268 immunohistochemistry protocol has been described elsewhere[22]. Briefly, rabbit anti-Zif268 primary antibody (1:1,000; Santa Cruz Biotechnology, Santa Cruz, CA, USA, ref: Sc-189) was combined with biotinylated goat anti-rabbit antibody (1:200; Vector Laboratories, Burlingame, CA, USA). Olfactory bulb sections were then processed through an avidin–biotin–peroxidase complex (ABC Elite Kit, Vector Laboratories). Following dehydration in graded ethanols, sections were defatted in xylene and coverslipped in DPX (Fluka, Sigma).

Zif268$^+$cell mapping. For each animal (n = 16 mice for unpleasant odorants (Guai, n = 4; ThioA, n = 3; Pyr, n = 3; Hex, n = 2; Cres, n = 4) and n = 16 for pleasant odorants (Lim, n = 2; Cam, n = 3; Cine, n = 5; Citro, n = 3; Ion, n = 3)), Zif268 immunohistochemistry was performed on adjacent olfactory bulb sections. Immuno-positive cells were counted on 21 sections (14 µm thick, 70 µm intervals) of the right olfactory bulb. All cell counts were conducted blind with regard to the experimental group. Within each section analyzed, Zif268 immuno-positive cells were automatically detected in the granule cell layer and the glomerular layers using mapping software (Mercator, Explora Nova, La Rochelle, France) coupled to a Zeiss microscope.

Two-dimensional olfactory bulb map building. Building an immuno-positive-cell density map has already been described[15]. Briefly, the granule and glomerular cell layers were divided into 36 sectors of 10° each, with a reference axis drawn parallel to the most ventral aspect of the subependymal layer of the olfactory bulb. For each layer, this segmentation yielded 756 bins (36 sectors × 21 sections) for which cell density (number of immuno-positive cells/mm^2) was calculated as shown in **Figure 2c**. Density values for each layer were then merged into a 2D map in which each column represents one section and each bin one sector. The columns were then aligned across animals using the most rostral aspect of the accessory olfactory bulb as an anatomical landmark.

Aligned individual maps were averaged within each group (low- or high-attractiveness odorants). A colored image plot of the data was constructed using Matlab 2015.

To provide an activity map more representative of the olfactory bulb, the bins were rearranged in a profile view scaled to the size of the sections. To do so, homologous sectors of the lateral and medial sides were averaged and the density value thus obtained was reported on a map in which the bins were positioned up for dorsal and down for ventral on a lateral view of the olfactory bulb (**Supplementary Fig. 3**).

Analysis of olfactory bulb maps. *Point-by-point map comparisons.* Comparisons of the distribution of immuno-positive cell density between the groups exposed to low- and high-attractiveness odorants were performed in each layer (granule and glomerular cell layers) using a Mann-Whitney U test; each group contained 5 odors × 2–5 animals per odor). More precisely, a sliding area successively centered on each bin and covering 4 adjacent bins (2 × 2 bins around the central bin) was used and statistical significance was set at $P < 0.05$. After FDR correction, bins still showing significant differences between groups were color-coded and an image plot was constructed using Matlab. FDR-corrected Mann-Whitney comparisons were also done in artificial groups composed of 50% of animals exposed to high-attractiveness odorants and to 50% of low-attractiveness odorants. 300 different artificial-group pairs were tested. For eight regions of the olfactory bulb (4 (ventral glomerular, ventral granular, dorsal glomerular, dorsal granular) × 2 (anterior and posterior olfactory bulb)), the surface represented by significant bins was calculated as well as the proportion of total surface it represents. t-tests for comparison of proportions were applied to compare anterior and posterior regions (**Supplementary Tables 2** and **3**).

Contrasting the hotspots for high- and low-attractiveness odorants. Here, we searched for bins of activation common to the five odorants of one group but not shared with the five odorants of other group, in other words, bins specifically activated by one group of odorants. To do this we first averaged the maps obtained for each odorant across animals (n = 2 to 5 animals per odor). These maps were then binarized to keep only the 20% of bins with the highest Zif268 density (activation hotspots, value = 1, everywhere else value = 0). An overlap map reflecting the activation hotspots for high-attractiveness odors was then calculated by summing these threshold-based odor maps. In this overlap map, a bin with a value of 0 indicated no strong activation in any of the five high-attractiveness odor maps. Conversely, a bin with a value of 5 indicates that this bin was highly activated in all five odor maps. The same protocol was applied to build the low-attractiveness overlap map.

Finally, subtracting the high-attractiveness overlap map from the low-attractiveness overlap map enabled us to highlight hedonic hotspots.

Code availability. Sliding Mann-Whitney tests, overlaps and artificial group simulation in **Figure 2** and **Supplementary Figure 3** required custom Matlab codes that are provided in **Supplementary Software**.

Optogenetic experiment. *Virus infusion and optical fiber implantation in the olfactory bulb.* Prior to surgery, 55 mice were anaesthetized with an intraperitoneal cocktail injection of 50 mg/kg ketamine and 7.5 mg/kg xylazine and secured in a stereotaxic instrument (Narishige Scientific Instruments, Tokyo,

Japan). 150 nl of pLenti-hSyn-eNpHR3.0-EYFP lentivirus (9,22 × 10^6 IU/ml, expressing halorhodopsin and the yellow fluorescent protein) and 300 nl of control pLenti-hSyn-EYFP lentivirus (1,1 × 10^6 IU/ml, expressing only YFP) were injected bilaterally into the posterior olfactory bulb (with respect to the bregma: AP, +4.3 mm; ML, ± 0.75; DV, −2 mm) or anterior olfactory bulb (with respect to the bregma: AP, +5 mm; ML, ± 0.75; DV, −2 mm) at a rate of 150 nl/min. Following virus infusions, a dual optical fiber (200-nm core diameter, 0.22 N.A.; Doric Lenses) was implanted into the olfactory bulb at the same coordinates as the virus infusion.

The pLenti-hSyn-eNpHR 3.0-EYFP was a gift from Karl Deisseroth[23] and obtained through Addgene (plasmid #26775). The control pLenti-hSyn-EYFP lentivirus (empty virus containing only the EYFP insert) was obtained from the pLenti-hSyn-eNpHR 3.0-EYFP plasmid by PCR amplification of the EYFP sequence and insertion into the pLenti-hSyn-eNpHR 3.0-EYFP backbone by recombination (In-fusion cloning kit, Clontech).

Optical stimulation in freely moving animals. Animals injected with the lentivirus into the posterior granule cell layer and implanted with optical fibers 8–10 weeks beforehand performed the 2-min olfactory preference test for the 5 unpleasant odorants (60 µl of pyridine, thioglycolic acid, 3-hexanol, guaiacol and *p*-cresol at 1 Pa; $n = 20$ mice) and the 5 pleasant odorants (60 µl of camphor, limonene, β-ionone, citronellol and cineole at 1 Pa, $n = 20$ mice). One odorant was tested per d. All mice were also tested in a no-odor condition. Bilateral continuous light stimulation (crystal laser, 561 nm, 10–15 mW) was automatically triggered when the mouse's nose came within 1 cm of the hole (VideoTrack, Viewpoint) and stopped automatically when the nose exited the zone. Total duration of nose-poking into the hole (odor investigation time) was used as a measure of odor preference. Animals injected with lentivirus into the anterior granule cell layer were subjected to the same behavioral test. Investigation time between the control and NpHR mice was compared using Mann-Whitney tests. Behavioral experiments were conducted blind with regard to the experimental group (control versus NpHR). Nine trials out of 240 were discarded because unwanted events during testing disturbed the animals.

Control of light-triggered inhibition. A few days after the olfactory preference testing, all mice were light stimulated (5 s of light stimulation every 15 s for 2 min at 10–15 mW, mimicking the light stimulation received during the preference test) one hour before euthanasia. Each mouse olfactory bulb was coronally sectioned (14 µm). EYFP (inhibitory channel expressing cells) and Zif268 double staining was performed on olfactory bulb sections as described previously (incubation with rabbit Zif268 antibody (1:1,000, Santa Cruz, ref: Sc-189), chicken GFP antibody (1:1,000, Anaspec TEBU, ref: 55423) and guinea pig Tbx21 (1:5,000, gift from Y. Yoshihara). The density of EYFP, Zif268$^+$ and the percentage of double-stained cells were counted in the ventral olfactory bulb on 2–4 sections (inter section interval = 70 µm) covering 140–280 µm under the injection site and at a distance from it (about 500 µm anterior or posterior depending on the injection site). As a control, YFP$^+$ cells were also assessed in the dorsal olfactory bulb. Positive cell densities or percentages of double stained cells were calculated for each animal, averaged within groups and compared using Wilcoxon tests. Assessment of cell density experiments were conducted blind with regard to the experimental group. In some cases, histology was not sufficiently well preserved to efficiently perform cell counts ($n = 5$ mice discarded).

In addition, we did slice recording on granule cells: animals infused in the olfactory bulb with NpHR ($n = 5$) or the control virus ($n = 3$) (with respect to the bregma: AP, +4.3 mm; ML, ± 0.75; DV, −2 mm; $n = 5$) 8 weeks earlier were anaesthetized with an intra-peritoneal injection of ketamine (50 mg/ml) and decapitated. The head was quickly immersed in ice-cold (2–4 °C) carbogenated artificial cerebrospinal fluid (cACSF; composition: 125 mM NaCl, 4 mM KCl, 25 mM $NaHCO_3$, 0.5 mM $CaCl_2$, 1.25 mM NaH_2PO_4, 7 mM $MgCl_2$ and 5.5 mM glucose; pH = 7.4) oxygenated with 95% O_2/5% CO_2. The osmolarity was adjusted to 320 mOsm with sucrose. Olfactory bulbs were removed and cut in horizontal slices (400 µm thick) using a Leica VT1000s vibratome (Leica Biosystems, France). Slices were incubated in a Gibb's chamber at 30 ± 1 °C using an ACSF solution with a composition similar to the cACSF, except that the $CaCl_2$ and $MgCl_2$ concentrations were 2 mM and 1 mM, respectively.

Slices were transferred to a recording chamber mounted on an upright microscope (Axioskop FS, Zeiss) and were continuously perfused with oxygenated ACSF (4 ml/min) at 30 ± 1 °C. Granule cells expressing the EYFP were visualized using an epifluorescence microscope (Zeiss Axio Scope) with a 40× objective (Zeiss Plan-Apochromat) and the bandpass filters set 38HE (Zeiss, excitation 470/40 nm, emission 525/50 nm). The illumination was produced by a white LED (Dual Port OptoLED, Cairn Research, UK). Measurements were performed with an RK 400 amplifier (BioLogic, France). The data were acquired with a sampling frequency of 20 kHz on a PC-Pentium D computer using a 12-bit A/D-D/A converter (Digidata 1440A, Axon Instruments) and PClamp10 software (Axon Instruments). Patch-clamp configurations were achieved with borosilicate pipettes (o.d.: 1.5 mm; i.d.: 1.17 mm; Clark Electromedical Instruments). The recording pipette was filled with the following intracellular solution (131 mM K-gluconate, 10 mM HEPES, 1 mM EGTA, 1 mM $MgCl_2$, 2 mM ATP-Na_2, 0.3 mM GTP-Na_3 and 10 mM phosphocreatine; pH = 7.3, 290 mOsm). Halorhodopsin was excited at 470–570 nm.

Activated mitral cells were assessed using labeling with Zif268 (1:1,000, Santa Cruz, ref: Sc-189) and Tbx21 (1:5,000, a gift from Y. Yoshihara), a specific marker of mitral cells. Double-labeled cells were counted in the dorsal and the ventral parts of the OB.

In the olfactory bulb slices prepared from the mice as described above (control $n = 3$ mice and $n = 6$ cells, NpHR, $n = 4$ mice and $n = 6$ cells), the spontaneous firing activity of the mitral cells was recorded in a cell-attached configuration. 5-s recordings in the control condition were alternated with 5 s in the presence of LED illumination (between 6 and 10 recording sessions for each condition). The effect of light stimulation was compared between NpHR and the control mice.

Statistics. A Kolmogorov-Smirnov test was used to assess normality of the data. Due to differences in normality across the different data sets, we chose to use Mann-Whitney tests, permutation tests or Wilcoxon tests for paired data (Statistica) in this study. No statistical methods were used to predetermine sample sizes, but our sample sizes were similar to those reported in previous publications[14,21,24,25]. Data collection and animal assignation to the various experimental groups were randomized.

A **Supplementary Methods Checklist** is available.

Data availability. The data that support the findings of this study are available from the corresponding author upon request.

20. Cleland, T.A., Morse, A., Yue, E.L. & Linster, C. *Behav. Neurosci.* **116**, 222–231 (2002).
21. Mandairon, N., Sultan, S., Nouvian, M., Sacquet, J. & Didier, A. *J. Neurosci.* **31**, 12455–12460 (2011).
22. Busto, G.U. *et al. Eur. J. Neurosci.* **29**, 1431–1439 (2009).
23. Gradinaru, V. *et al. Cell* **141**, 154–165 (2010).
24. Moreno, M.M. *et al. Proc. Natl. Acad. Sci. USA* **106**, 17980–17985 (2009).
25. Sultan, S., Rey, N., Sacquet, J., Mandairon, N. & Didier, A. *J. Neurosci.* **31**, 14893–14898 (2011).

doi:10.1038/nn.4317